JOURNAL OF NANO AND MATERIAL SCIENCE RESEARCH
Volume 1 (Maiden edition, 2022), pp. 9-15
Available online at journals.nanotechunn.com/jnmsr

ORIGINAL ARTICLE

Synthesis and Characterization of SILAR-Deposited Leaf-Like Copper Sulphide Films

*C.F. Ugbo[a], A.C. Nkele[a], A. Agbogu[a], A.B.C. Ekwealor[a], M. Maaza[b,c], A.C. Nwanya[a,d], R.U. Osuji[a,b,c], F.I. Ezema[a,b,c,d]**

[a]*Department of Physics and Astronomy, University of Nigeria, Nsukka Enugu State, Nigeria.*
[b]*Nanosciences African Network (NANOAFNET) iThemba LABS-National Research Foundation, 1 Old Faure Road, Somerset West 7129, P.O. Box 722, Somerset West, Western Cape Province, South Africa.*
[c]*UNESCO-UNISA Africa Chair in Nanosciences/Nanotechnology, College of Graduate Studies, University of South Africa (UNISA), Muckleneuk Ridge, P. O. Box 329, Pretoria, South Africa*
[d]*Africa Centre of Excellence for Sustainable Power and Energy Development (ACE-SPED), University of Nigeria, Nsukka 410001, Nigeria*

KEYWORDS

Copper sulphide, SILAR Orthorhombic, Band gap, Supercapacitors

ARTICLE HISTORY

Received: July 3, 2022
Revised: July 18, 2022
Accepted: August 2, 2022

ABSTRACT

Successful synthesis of copper sulphide films deposited via successive ionic layer adsorption and reaction (SILAR) method at 100, 150, and 200 cycles. The deposited films were characterized for their morphological, structural, elemental, optical, and electrochemical features. A leaf-like morphology was obtained for the CuS films. Orthorhombic crystal structure with distinct peaks at (262) and (116) planes were observed. Good optical features, high absorbance with band gap energies ranging from 1.95 eV to 1.98 eV. The synthesized films possessed good electrochemical features with supercapacitive abilities. The synthesized materials find potential applications in optical devices and supercapacitors.

1 Introduction

A major concern for researchers and scientists in the world today is obtaining sustainable energy that will address the issue of global warming, pollution, and help prevent the production of CO_2 which poses a threat to human life [1]. Renewable energy sources, on the other hand, are alternative and sustainable sources that are natural, abundant, green, and renewable.

Researchers and scientists delved into an extensive study on supercapacitors owing to their usefulness and wide range of applications, not only in storage devices but also in making energy readily available especially in remote areas [1]. Their business is to produce high power density but they are deficient in the production of energy density in respect to batteries [2]. Supercapacitors or ultracapacitors keep electrical energy by dual means: double-layer capacitance (electrostatic storage process) or pseudocapacitance (Faradaic redox storage process) [3]. Many years of research have shown that acidic and alkaline electrolyte solutions produce high specific capacitive materials while organic electrolyte yields high operating voltage [4]. Several compounds such as CoS, CuS, MnS, and NiS have been proven to be good electrode materials for supercapacitors [5] because of the sulfur content that is rich in energy density, and different oxidation states which support reversible redox reaction in energy storage devices [6].

Copper sulfide is a p-type semiconductor known for its high extinction coefficient, high refractive index, specific capacitance, band gap, and high conductivity which makes it of great interest to the optoelectronic [7], catalytic [8], and gas sensing [9] industries. Diverse processes have been adopted in fabricating CuS such as successive ionic layer adsorption and reaction (SILAR), chemical bath deposition (CBD), sol-gel, atomic layer deposition, spray pyrolysis [9], etc. In SILAR

*CORRESPONDING AUTHOR | F.I. Ezema | ✉fabian.ezema@unn.edu.ng

process, the film is prepared by dipping the glass slide into cationic and anionic precursor solutions with rinsing in the middle to remove the unbounded ions. SILAR method was employed because it is an affordable and easy synthesis process, for depositing material at low temperatures, for fabricating flexible photovoltaic devices.

Copper sulfide films have been deposited on glass substrates using cupric sulfate and sodium sulfide aqueous solutions as precursors on glass substrate by SILAR method at room temperature with an obtained band gap energy of 2.14 eV [10]. The CBD method was also utilized in growing CuS thin films on glass substrates at 300 K with band gap energies ranging from 1.60 to 2.40 eV [11]. SILAR method was also used to prepare CuS films from solutions of $CuCl_2$ and Na_2S at two different molarities on glass substrates at room temperature with the band gap energy found to vary from 2.2 to 2.8 eV.

This work focuses on studying the effects of varying deposition cycles on SILAR-deposited CuS films using thioacetamide as the anionic precursor. The morphological, structural, elemental, optical, and electrochemical features of the deposited films have been discussed.

2 Experimental details

2.1 Synthesis of CuS film

Before the deposition, the substrates were washed with clean water, put in acetone for 25 minutes, rinsed in distilled water, placed in an ultrasonicator for 25 minutes, and dried in an oven set at 60℃ for 15 minutes. The substrates were weighed and kept in a neat container as the precursor solutions were prepared.

For the cationic precursor solution, 0.21 M of cupric sulfate ($CuSO_4$) was mixed with 50 ml of distilled water and stirred for 10 minutes. 0.03 M of sodium thiosulphate ($Na_2S_2O_3$) was dissolved in 50 ml of distilled water and stirred for 5 minutes. The solutions were mixed and stirred continuously, with 1 ml of NH_3 added dropwise to maintain the solution at a pH of 6.

For the anionic precursor solution, 0.025 M of thioacetamide (C_2H_5NS) was dissolved in 50 ml of distilled water and stirred for 5 minutes. A weighted and cleaned glass slide was placed in the cationic precursor for 10 seconds to allow the adsorption of Cu^{2+}, rinsed in the first beaker of distilled water for 5 seconds to remove the unbounded ions, placed in the anionic precursor for 10 seconds to allow reaction with S^{2-}, and finally rinsed in distilled water for 5 seconds to remove the infirmly bonded ions.

The same procedures were taken to deposit the CuS on stainless steel substrates. The process was repeated for 100, 150, and 200 cycles at room temperature and annealed at 200℃ for 1 hour. The films were weighed before and after deposition to provide for thickness values. The processes involved in the deposition of the CuS films are described by Figure 1 with the arrowhead giving the sequence of deposition.

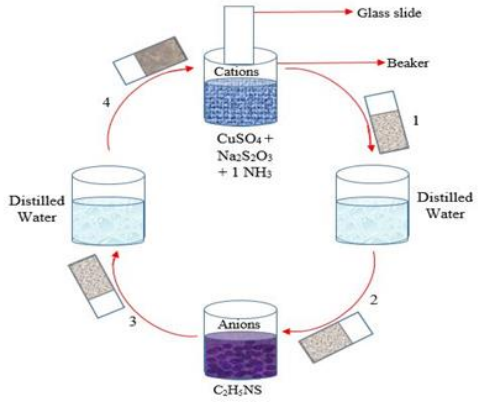

Figure 1: Schematic of a 4-beaker cyclic SILAR process for CuS films

2.2 Characterization Techniques

The synthesized films were characterized for their morphological, structural, elemental, optical, and electrochemical features using Zeiss scanning electron microscope, Siemens X-ray diffractometer, energy dispersive X-ray spectroscope (EDX), Shimadzu double beam spectrophotometer of model: UV–1800 in the wavelength range (200-1000 nm), and a Princeton applied research VersaSTAT potentiostat in a 3-electrode system respectively. The film thickness was measured using the gravimetric weight difference method.

3 Results and Discussions

3.1 Surface morphology study

It is very important to study the surface characteristics of CuS film since the charge storage in a supercapacitor is surface-oriented**.** Figure 2a-c exposes the surface images of the CuS films deposited at different cycles.

The film deposited at 100 cycles contains irregular microspheres, pores, and rod-like features scattered over the surface of the substrate. This porosity exhibited by the film enables redox interaction to occur [12].

A clear change in the surface formations of the film is seen as the deposition cycle increased to 150. The irregular microspheres became larger and were scantily scattered over the surface. The wider pores together with the irregular microspheres are suitable for supercapacitor applications because ions in the electrolyte easily reach the microsphere and increase redox activity on the surface of the CuS film.

More so, as the number of cycles increased further to 200, the morphology was transformed to flower-like agglomerated features which clustered at the center of the substrate showing increased redox interaction [13].

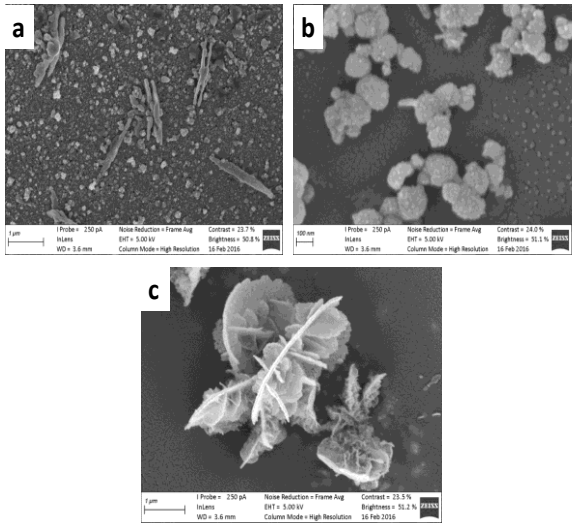

Figure 2: SEM images of CuS films deposited at a) 100 b) 150 and c) 200 cycles

3.2 Structural study

XRD is an indispensable tool in crystal structure analysis because it produces information about the phase structure of the material. The Cu_xS orthorhombic phase structure corresponds to the JCPDS card number: 23-0961. Two crystalline peaks were prominently observed in Figure 3 at (262) and (116) planes for the CuS films deposited at 150 and 200 cycles.

It is interesting to know that the film deposited at 100 cycles did not yield any prominent crystalline peak; probably because the deposition time was not sufficient to transform the phase of the material [14]. As the number of deposition cycles increased, more peaks were produced due to the accumulation of more ions on the surface of the material. This is in proper alignment with the previous report [15].

Additionally, the peaks produced by the 150 and 200 cycles deposited films could have resulted from the effect of deposition time since the films were subjected to the same annealing conditions.

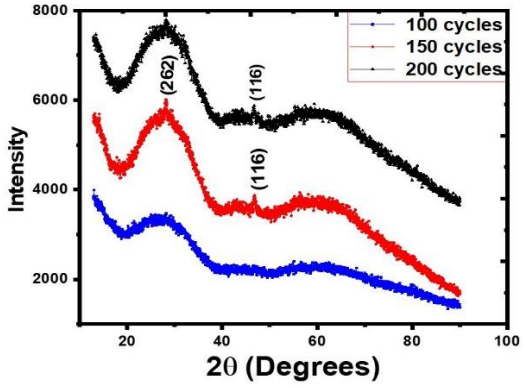

Figure 3: XRD patterns of the CuS films synthesized at a) 100 b) 150 and c) 200 cycles

3.3 Elemental composition

Figure 4a-c displays a set of EDX spectra for the deposited CuS films.

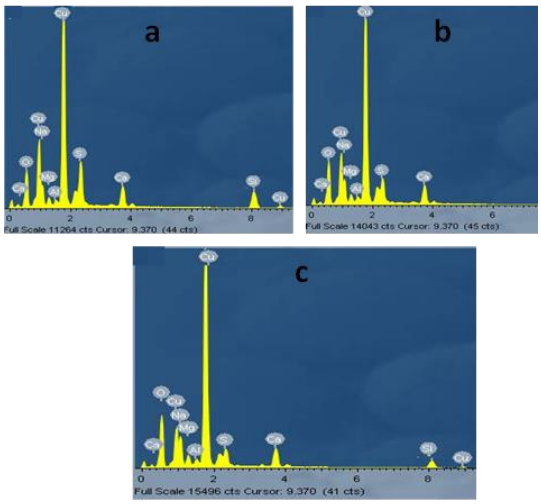

Figure 4: EDX spectra of the CuS films deposited at a) 100 b) 150 and c) 200 cycles

There exist a very high peak of copper (Cu) and shorter peaks of sulfur (S) along with other elements such as silicon (Si), calcium (Ca), and sodium (Na) which originated from the glass substrate and is noticeable in all the deposited materials.

Oxygen (O) emanated as a result of the reaction between the CuS electrode and the atmosphere. It can be observed that the films in each of the cycles showed the same pattern of peaks indicating the uniform distribution of the CuS electrode on the glass slides. The presence of peaks of Cu and S confirms the deposition of CuS film on the substrate.

3.4 Optical studies

Figure 5a shows the absorbance in (%) of CuS plotted against wavelength in (nm) for the films deposited at 100, 150, and 200 cycles at room temperature. The spectra revealed a high absorption in the visible region with the absorption edge within 300 and 450 nm. There exists an exponential decay by the absorption as the wavelength increased from 450-850 nm brought about by annealing treatment given to the samples [14].

The broad absorbance in the visible region indicates that the CuS electrode is a desirable candidate for pseudocapacitor. It is important to note here that the film deposited at 200 cycles showed the highest peak followed by 150 and 100 cycles. Hence, we can say that the number of deposition cycles affected the absorbance of the films. Therefore, the thicker the film, the more the ions inside the film absorb UV radiation [16,17].

From Figure 5b, annealing the films increased the optical transmittance, this increment could be attributed to the decreasing and rearrangement defects of the films. In addition, the annealing led to improvement of crystallinity of the film's

structure [16,18,19]. Therefore, CuS thin films can be used as transparent conducting material [11].

Figure 5c shows the reflectance curves for CuS films deposited at 100, 150, and 200 cycles. There is an exponential growth in the percentage reflectance of the films with the wavelength. The peak reflectance was noticed by the film at 200 cycles while the least was at 100 cycles. It is evident that at higher cycles, the film was very thick, hence could not reflect much UV radiation.

Again, all the films had high reflectance in the NIR regions at wavelengths of 800 nm and 1000 nm. The low reflectance possessed by CuS in the visible region makes it suitable as a coating material.

Figure 6 gives a graph of $(\alpha h\nu)^2$ plotted against hν. The intercept of the graph was traced along the photon energy axis and the results obtained from the graph are 1.95 eV, 1.97 eV, and 1.98 eV for 100, 150, and 200 cycles respectively.

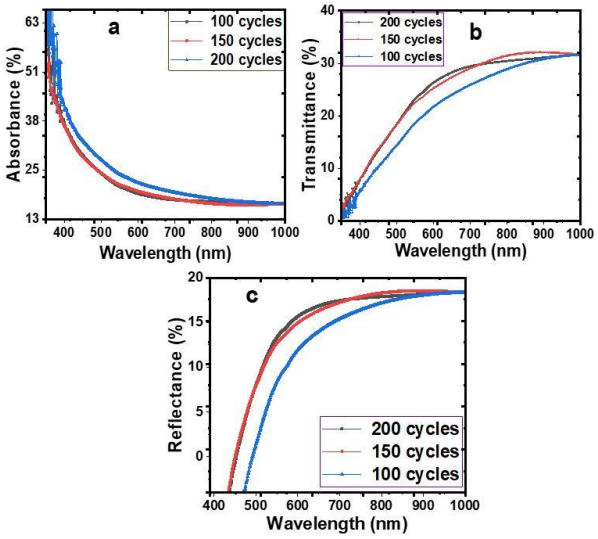

Figure 5: Optical a) absorbance b) transmittance and c) reflectance plots of the CuS films

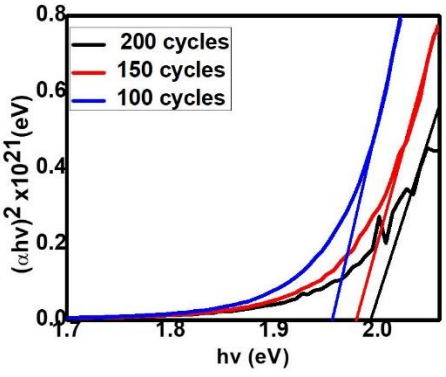

Figure 6: Energy band gap plots of the CuS films

It is very crucial to note here that, increase in the deposition cycle led to increase in the band gap. This is because, at higher number of deposition cycles, more ions are available on the film surface resulting in the absorption of UV radiation that is just enough to excite the electrons**.** The band gap result shows that the CuS is a good material for the fabrication of solar cells. This kind of report was also obtained by [20].

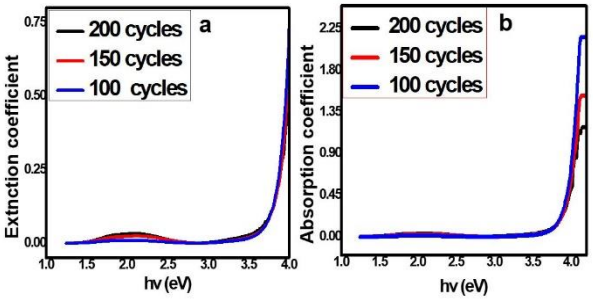

Figure 7: Extinction coefficient and b) absorption coefficient plots of the CuS films

The extinction coefficient (k) refers to the quantity of absorbed energy in the film. The decrease in 'k' was due to the variation in the absorbance. The extinction coefficient in Figure 7a increases with an increase in the photon energy and decreases with an increase in wavelength.

The hump signifies that the deposited CuS films absorbed a reasonable amount of optical energy. Since k decreases with increasing wavelength, it shows that the transparent films seem to behave like transparent insulators, preventing high energy UV and high energy temperature NIR radiation into a building while allowing only visible light [21].

The graph of optical absorption coefficient, α vs photon energy, hν is shown in Figure 7b for the CuS films. The films have a high absorption coefficient that means all films have direct band gap energy. The minimum is value is 0.01 which occurred at 1.2 eV and the maximum value lies between 2.2 at 3.7 eV.

As depicted in Figure 8a, the optical conductivity increased linearly and almost equally with photon energy up to about 3.52 eV. The slope of the curve changed with each cycle until a peak was reached at 3.76, 3.8, and 3.83 eV for 200, 150, and 100 cycles. After this peak, there was a sharp decay in the conductivity graph.

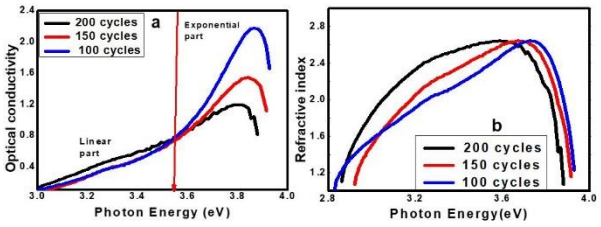

Figure 8: a) Optical conductivity and b) Refractive index plots of the CuS films

These two different slopes indicate that the conductivity is governed by two mechanisms. In the linear part, the conductivity is proportional to photon energy. After 3.52 eV

(exponential part), electrons produced probably have enough energy to ionize other atoms leading to the production of electron-hole pairs which eventually leads to an exponential increase in conductivity. It is pertinent to stress here that the decrease after the peaks was probably due to recombination.

3.5 Electrochemical studies

The electrochemical analysis is an important way of obtaining the chemical properties of the material with respect to the potentiometer and the electrolyte. To check the electrochemical performance of CuS as a powerful electrode material for supercapacitor, the cyclic voltammetry (CV) and the electrochemical impedance spectroscopy (EIS) techniques were employed.

Usually, in a typical electrochemical analysis, the material synthesized is the working electrode, the Ag/AgCl is known as the reference electrode while the graphite is the counter electrode in a 3-electrode system.

3.5.1 Cyclic Voltammetry (CV) analysis

Cyclic voltammetry among other analytical techniques is the most popular technique that discloses information about the electrochemical processes occurring at the interface of the electrochemical cell and the material. The cyclic voltammogram displays the plot of the current density (s) as a function of the potential (V).

Figure 9a-c shows the cyclic voltammetry (CV) plots carried out between -1 to +1 V vs Ag/AgCl at scan rates of 50, 100, 150, and 200 mV/s in the presence of 1 M of potassium hydroxide (KOH) solution at room temperature for the CuS electrodes produced at 100, 150, and 200 cycles.

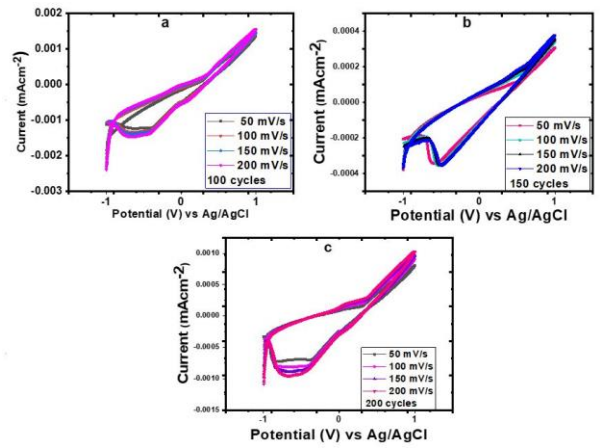

Figure 9: Cyclic voltammograms of the CuS electrodes

The shapes of the curve produced for all the materials are rectangular, indicating that CuS is good pseudocapacitive material [13]. The materials produced at 150 cycles possess wider rectangle curves indicating higher capacitance [14]. Additionally, there were no noticeable redox peaks in all the deposited electrode suggesting high stability and good reversibility of CuS [22]. Specific capacitance was obtained from the CV by applying equation (1) [23–25] given as:

$$C_s = \frac{\int I\, dV}{m_2 - m_1 * V_f - V_i * (V)} \quad (1)$$

Here, m_1 and m_2 are masses before and after deposition of the films, (V_f and V_i) is the potential range from which the analysis was done that is, (-1.0 to +1.0 V vs Ag/AgCl), I represents the current density ($mAcm^{-2}$), V is the scan rate and $\int dv$ represents the area under the CV curve.

The graph of the specific capacitance against the scan rate for the CuS electrode deposited at different cycles is well represented in Figure 10. From the graph, it was noticed that the specific capacitance experienced decay for all the electrodes when the scan rate was constantly increasing. This is a behavior often associated with supercapacitors owing to their dependence on charge and discharge current and frequency [13].

The dependency of the frequency could be attributed to the departure between the electrode and the ions. The highest specific capacitance 15.497 Fg^{-1} was obtained at the lowest scan rate 50 mVs^{-1} with the material at 200 cycles. This is a result of the cooperation between more ions present in the electrode compared to other cycles. A similar result was reported by [13] for a good supercapacitor material.

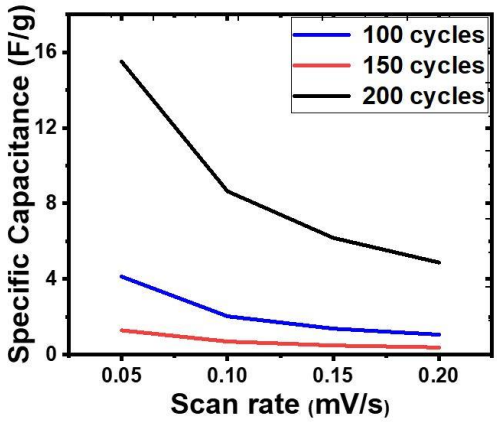

Figure 10: Plot of specific capacitance against scan rate for the CuS electrodes

The Nyquist plot usually represents the plot of the Z_{im} (Ohms) against the Z_{real} (Ohms). It is employed in the EIS analysis because it provides a very useful means of checking the qualities of the charge carrier in a material [26].

Figure 11 represents the Nyquist diagrams of the CuS films deposited at different cycles at room temperature in the presence of 1 M of KOH solution at a potential range of -1.0 to +1.0 V vs Ag/AgCl. The films exhibit interesting curves having two sections. The first part resembles a semicircle which is located at the high-frequency region.

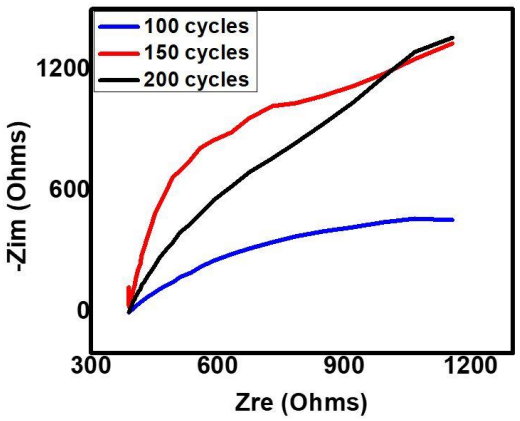

Figure 11: Nyquist plots of the CuS electrodes

This behavior is common with the double-layer capacitor. While the second was found at the vertical part at the low-frequency area, there was a reasonable difference in the behavior of the films. This difference in behavior could have emerged from the KOH electrolyte used [27]. This behavior is often associated with pseudocapacitance material.

4 Conclusion

This work successfully demonstrates the synthesis of copper sulfide films deposited via successive ionic layer adsorption and reaction (SILAR) method at 100, 150, and 200 cycles. All the films were annealed at 200℃ for I hour after deposition. The deposited films were characterized for their morphological, structural, elemental, optical, and electrochemical features using a scanning electron microscope, X-ray diffractometer, energy dispersive x-ray diffractometer, UV-vis spectrophotometer, and a 3-electrode potentiostat.

A leaf-like morphology was obtained for the CuS films while the structural studies revealed orthorhombic crystal structure with distinct peaks at (262) and (116) planes observed. The CuS films exhibited good optical features, high absorbance with band gap energies ranging from 1.95 eV to 1.98 eV. The synthesized films possessed good electrochemical features with supercapacitive abilities. The synthesized materials find potential applications in optical devices and supercapacitors.

Acknowledgements

The authors acknowledge the support by TETFUND under the contract number: TETFUND/DR&D/CE/UNI/NSUKKA/RP/VOL.I. FIE acknowledges the support received from the Africa Centre of Excellence for Sustainable Power and Energy Development (ACE-SPED), University of Nigeria, Nsukka.

Declaration of Competing Interest

The authors declare no conflict of interest in the funding of this work.

References

1. R. B. Pujari, A. C. Lokhande, A. R. Shelke, and C. D. Lokhande, "Novel chemical synthesis of sulfur thin film for supercapacitor application," Korea **500**, 757 (n.d.).
2. M. Jayalakshmi and K. Balasubramanian, "Simple Capacitors to Supercapacitors - An Overview," Int. J. Electrochem. Sci. **3**, 23 (2008).
3. G. S. Gund, D. P. Dubal, S. S. Shinde, and C. D. Lokhande, "Architectured Morphologies of Chemically Prepared NiO/MWCNTs Nanohybrid Thin Films for High Performance Supercapacitors," ACS Appl. Mater. Interfaces **6**(5), 3176–3188 (2014).
4. M. C. Nwankwo, A. C. Nwanya, A. Agbogu, A. B. C. Ekwealor, P. M. Ejikeme, R. Bucher, R. U. Osuji, M. Maaza, and F. I. Ezema, "Electrochemical supercapacitive properties of SILAR-Deposited Mn3O4 electrodes," Vacuum **158**, 206–214 (2018).
5. K.-J. Huang, L. Wang, Y.-J. Liu, Y.-M. Liu, H.-B. Wang, T. Gan, and L.-L. Wang, "Layered MoS2–graphene composites for supercapacitor applications with enhanced capacitive performance," International Journal of Hydrogen Energy **38**(32), 14027–14034 (2013).
6. X. Cui, Z. Shan, L. Cui, and J. Tian, "Enhanced electrochemical performance of sulfur/carbon nanocomposite material prepared via chemical deposition with a vacuum soaking step," Electrochimica Acta **105**, 23–30 (2013).
7. S. Gorai, D. Ganguli, and S. Chaudhuri, "Shape selective solvothermal synthesis of copper sulphides: role of ethylenediamine–water solvent system," Materials Science and Engineering: B **116**(2), 221–225 (2005).
8. A. E. Raevskaya, A. L. Stroyuk, S. Ya. Kuchmii, and A. I. Kryukov, "Catalytic activity of CuS nanoparticles in hydrosulfide ions air oxidation," Journal of Molecular Catalysis A: Chemical **212**(1), 259–265 (2004).
9. P. Baláž, L. Takacs, E. Boldižárová, and E. Godočíková, "Mechanochemical transformations and reactivity in copper sulphides," Journal of Physics and Chemistry of Solids **64**(8), 1413–1417 (2003).
10. A. Astam, Y. Akaltun, and M. YILDIRIM, "An investigation on SILAR deposited Cu_xS thin films," Turkish Journal of Physics **38**(2), 245–252 (2014).
11. F. I. Ezema, M. N. Nnabuchi, and R. U. Osuji, "Optical properties of CuS thin films deposited by chemical bath deposition technique and their applications," Trends in Applied Sciences Research **1**(5), 467–476 (2006).
12. Y. Sun, S. Wang, H. Cheng, Y. Dai, J. Yu, and J. Wu, "Synthesis of a ternary polyaniline@ acetylene black-

sulfur material by continuous two-step liquid phase for lithium sulfur batteries," Electrochimica Acta **158**, 143–151 (2015).

13. Y. Lu, X. Liu, W. Wang, J. Cheng, H. Yan, C. Tang, J.-K. Kim, and Y. Luo, "Hierarchical, porous CuS microspheres integrated with carbon nanotubes for high-performance supercapacitors," Scientific reports **5**, 16584 (2015).

14. A. H. O. Al-khayatt and M. D. Jaafer, "Annealing Effect on The Structural and Optical Properties of CuS Thin Film Prepared By Chemical Bath Deposition (CBD)," Journal of Kufa - physics **5**(1), 79–90 (2013).

15. B. N. Kakade, C. P. Nikam, and S. R. Gosavi, "Effect of immersion cycles on structural, morphology and optoelectronic properties of nanocrystalline Ag2S thin films deposited by SILAR technique," J. Appl. Phys **6**(6), 6–12 (2014).

16. A. M. Mousa and A. F. Sabbar, "Influence Of Post-Annealing On The Properties Of Cuxs: Al, Fe Films Deposited By CBD," Engineering and Technology Journal **27**(14), 2632–2641 (2009).

17. M. Xin, K. Li, and H. Wang, "Synthesis of CuS thin films by microwave assisted chemical bath deposition," Applied Surface Science **256**(5), 1436–1442 (2009).

18. S. B. Aziz, M. A. Rasheed, and H. M. Ahmed, "Synthesis of polymer nanocomposites based on [Methyl Cellulose](1− x):(CuS) x (0.02 M≤ x≤ 0.08 M) with desired optical band gaps," Polymers **9**(6), 194 (2017).

19. E. Güneri and A. Kariper, "Optical properties of amorphous CuS thin films deposited chemically at different pH values," Journal of Alloys and Compounds **516**, 20–26 (2012).

20. M. Saranya, C. Santhosh, R. Ramachandran, and A. Nirmala Grace, "Growth of CuS nanostructures by hydrothermal route and its optical properties," Journal of Nanotechnology **2014**, (2014).

21. S. U. Offiah, P. E. Ugwoke, A. B. C. Ekwealor, S. C. Ezugwu, R. U. Osuji, and F. I. Ezema, "Structural and spectral analysis of chemical bath deposited copper sulfide thin films for solar energy conversions," Digest Journal of Nanomaterials and Biostructures **7**(1), 165–173 (2012).

22. A. N. S. B. A. Metosen, C. P. Suh, and S. F. Chin, "Nanostructured multilayer composite films of manganese dioxide/nickel/copper sulfide deposited on polyethylene terephthalate supporting substrate," Journal of Nanomaterials **2015**, (2015).

23. B. N. Ezealigo, A. C. Nwanya, A. Simo, R. U. Osuji, R. Bucher, M. Maaza, and F. I. Ezema, "Optical and electrochemical capacitive properties of copper (I) iodide thin film deposited by SILAR method," Arabian Journal of Chemistry (2017).

24. A. C. Nwanya, S. U. Offiah, I. C. Amaechi, S. Agbo, S. C. Ezugwu, B. T. Sone, R. U. Osuji, M. Maaza, and F. I. Ezema, "Electrochromic and electrochemical supercapacitive properties of Room Temperature PVP capped Ni(OH)2/NiO Thin Films," Electrochimica Acta **171**, 128–141 (2015).

25. A. C. Nkele, A. C. Nwanya, N. U. Nwankwo, R. U. Osuji, A. B. C. Ekwealor, P. M. Ejikeme, M. Maaza, and F. I. Ezema, "Investigating the properties of nano nest-like nickel oxide and the NiO/Perovskite for potential application as a hole transport material," Adv. Nat. Sci: Nanosci. Nanotechnol. **10**(4), 045009 (2019).

26. S.-F. Chin, S.-C. Pang, and M. A. Anderson, "Material and electrochemical characterization of tetrapropylammonium manganese oxide thin films as novel electrode materials for electrochemical capacitors," Journal of the Electrochemical Society **149**(4), A379–A384 (2002).

27. G. Mula, M. V. Tiddia, R. Ruffilli, A. Falqui, S. Palmas, and M. Mascia, "Electrochemical impedance spectroscopy of oxidized porous silicon," Thin Solid Films **556**, 311–316 (2014).